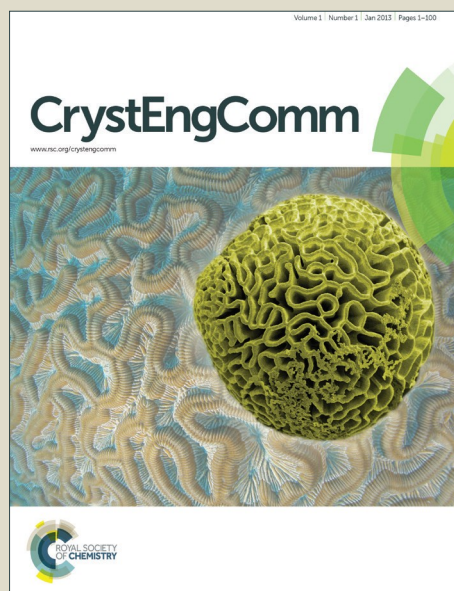


CrystEngComm

Accepted Manuscript



This article can be cited before page numbers have been issued, to do this please use: M. C. Aragoni, M. Arca, S. Coles, M. Crespo-Alonso, S. Coles, R. Davies, M. Hursthouse, F. Isaia, R. Lai and V. Lippolis, *CrystEngComm*, 2016, DOI: 10.1039/C6CE00991C.



This is an *Accepted Manuscript*, which has been through the Royal Society of Chemistry peer review process and has been accepted for publication.

Accepted Manuscripts are published online shortly after acceptance, before technical editing, formatting and proof reading. Using this free service, authors can make their results available to the community, in citable form, before we publish the edited article. We will replace this *Accepted Manuscript* with the edited and formatted *Advance Article* as soon as it is available.

You can find more information about *Accepted Manuscripts* in the [Information for Authors](#).

Please note that technical editing may introduce minor changes to the text and/or graphics, which may alter content. The journal's standard [Terms & Conditions](#) and the [Ethical guidelines](#) still apply. In no event shall the Royal Society of Chemistry be held responsible for any errors or omissions in this *Accepted Manuscript* or any consequences arising from the use of any information it contains.



Journal Name

ARTICLE

Coordination polymers and polygons using di-pyridyl-thiadiazole spacers and substituted phosphorodithioato Ni^{II} complexes: potential and limitations for inorganic crystal engineering

Received 00th January 20xx,
Accepted 00th January 20xx

DOI: 10.1039/x0xx00000x

www.rsc.org/

M. Carla Aragoni,^a Massimiliano Arca,^a Simon J. Coles,^b Miriam Crespo,^a Susanne L. Coles (née Huth),^c Robert P. Davies,^d Michael B. Hursthouse,^b Francesco Isaia,^a Romina Lai^a and Vito Lippolis^a

Coordinatively unsaturated P-substituted dithiophosphonato, dithiophosphato, and dithiophosphito complexes [Ni((MeO)₂PS₂)₂] (**1**), [Ni((EtO)₂PS₂)₂] (**2**), [Ni(MeOdtP)₂] (**3**), and [Ni((Ph)₂PS₂)₂] (**4**) were reacted with the *bis*-functional ligands 3,5-di-(4-pyridyl)-1,2,4-thiadiazole (**L1**) and 3,5-di-(3-pyridyl)-1,2,4-thiadiazole (**L2**) to give the coordination polymers (**1–4·L1**)_∞, (**3·L2**)_∞, (**4·L2·2C₇H₈**)_∞ and the discrete dimers (**1–2·L2**)₂, all characterised by single crystal X-ray diffraction. The comparison of the structures show that **L1** can be exploited for the predictable assembly of undulating chains independent of the nature of the Ni^{II} complex while **L2** allows for the existence of different supramolecular constructs ensuing from different ligand conformations deriving from the rotation of the pyridyl rings.

Introduction

The last decades experienced an impressive number of novel multidentate bridging ligands designed to construct a variety of discrete metal–organic polygons and polyhedra (MOPs), or metal–organic frameworks (MOFs) with high dimensionality. These supramolecular assemblies are of great appeal for a combination of their intrinsic beauty and promising applications in fields as varied as gas storage, ion exchange, chemical sensing, catalysis, energy transfer, and separation.^{1,†}

The properties of these crystalline materials are critically dependent on their network structures, and the deliberate creation of a crystalline network, planned using properly designed building blocks remains, nowadays, a challenge. Several aspects need to be evaluated in developing a network based on coordination polymers: the building blocks, i.e. metal nodes and organic spacers, metal coordination environments, formation conditions, and weak secondary interactions. Multi-topic organic molecules are commonly used as spacers and an opportune choice of the number and position of donor atoms

can be used to direct the network assembly, although factors such as flexibility of the ligand and different accessible conformations need to be examined and taken into account. The metal coordination environment is exceptionally difficult to control when “naked” metal ions are used as nodes and, in view of that, the use of neutral coordination complexes held together by additional donor molecules or secondary bonding interactions has gained striking importance.² In fact, by reducing the degrees of freedom of the system, for instance by using *cis*-protected metal blocks in place of the naked metal ions, or by using a neutral, coordinatively unsaturated metal complex, less uncertainty can be expected. Moreover, the use of neutral synthons leads to self-reliant supramolecular assemblies which do not require the presence of a counterion and thus reduce the occurrence of isomerism.

In this respect, we have been developing a synthetic program based on the ability of neutral dithiophosphonato Ni^{II} complexes [Ni(ROdtP)₂] [ROdtP = (RO)(4-MeOC₆H₄)PS₂[−]; R = alkyl substituent]³ to assemble coordination polymers in combination with a variety of polypyridyl donors, in particular 4,4'-bipyridine and its analogues.^{5,4} This assembly process is based on the capability of the coordinatively unsaturated Ni^{II} ion of these square-planar complexes to axially bind monodentate ligands, such as pyridine, to yield discrete octahedral complexes.^{5,6} In addition suitable N–L–N bidentate bipyridyl-based spacers yield 1D coordination polymers of the type [Ni(ROdtP)₂(N–L–N)]_∞.^{7,8} The primary structural motif of these polymers mainly depends on the features of the spacers such as length, rigidity and orientation of the donor atoms, as recently confirmed by the deliberate stereospecific generation of homochiral polymeric helices built from a designed enantiopure binaphthyl-based ligand.⁹

^a Dipartimento di Scienze Chimiche e Geologiche, Università degli Studi di Cagliari, S.S. 554 bivio per Sestu, 09042 Monserrato-Cagliari, Italy.
E-mail: aragoni@unica.it

^b EPSRC National Crystallography Service, School of Chemistry, University of Southampton, Highfield, Southampton SO17 1BJ, UK.

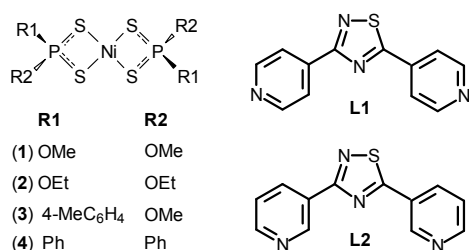
^c Department of Chemistry, Faculty of Natural and Environmental Sciences, University of Southampton, Highfield, Southampton SO17 1BJ, UK.

^d Department of Chemistry, Imperial College London, South Kensington, London, SW7 2AZ, U.K.

E-mail: r.davies@imperial.ac.uk

† Footnotes relating to the title and/or authors should appear here.

Electronic Supplementary Information (ESI) available: crystallographic data and figures for (**1–4·L1**)_∞, (**1–2·L1**)₂, (**3·L2**)_∞, and (**4·L2·2C₇H₈**)_∞. See DOI: 10.1039/x0xx00000x



Scheme 1 General scheme of complexes **1–4** (left) and ligands **L1–L2** (right).

The substituents on the phosphorus atoms are responsible for the connection of the polymers through hydrogen bonds and face-to-face or edge-to-face π - π interactions, thus influencing the final 3D-architecture.⁷ As a consequence, coordination polymers and 3D assemblies with different structures and architectures can be built up by varying either the bridging ligands or the substituents on the P atom of the initial Ni complexes. In order to better understand the process of molecular recognition between components and how the steric information contained in the P-substituents and in the orientation of ligand binding sites combine to give the final structure, differently P-substituted dithiophosphonato, dithiophosphato, and dithiophosphito complexes $[\text{Ni}((\text{MeO})_2\text{PS}_2)_2]$ (**1**), $[\text{Ni}((\text{EtO})_2\text{PS}_2)_2]$ (**2**), $[\text{Ni}(\text{MeOdtP})_2]$ (**3**), and $[\text{Ni}((\text{Ph})_2\text{PS}_2)_2]$ (**4**) were reacted with the bis-functional ligands 3,5-di-(4-pyridyl)-1,2,4-thiadiazole (**L1**)¹⁰ and 3,5-di-(3-pyridyl)-1,2,4-thiadiazole (**L2**)¹⁰ (Scheme 1).

We recently investigated the reactivity of **L1** and **L2** with I_2 and IBr , in both polar and apolar media, thereby elucidating the role of specific directional interactions, namely $\text{NH}^+\cdots\text{N}$ and $\text{N}\cdots\text{I}$, combined with geometrical features of the molecules, in the formation of different supramolecular constructs.¹⁰ The investigation of these ligands is extended here to the formation of coordination polymers.

Experimental

Materials

All commercially available compounds were used as received. Bis[O-alkyl-dithiophosphato]Ni complexes $[\text{Ni}((\text{RO})_2\text{PS}_2)_2]$ R = Me (**1**), Et (**2**),⁵ the dithiophosphonato Ni^{II} complex $[\text{Ni}(\text{MeOdtP})_2]$ [MeOdtP = $(\text{RO})(4\text{-MeOC}_6\text{H}_4)\text{PS}_2^-$],³ and bis-functional ligands 3,5-di-(4-pyridyl)-1,2,4-thiadiazole (**L1**) and 3,5-di-(3-pyridyl)-1,2,4-thiadiazole (**L2**),¹⁰ were synthesised according to previously reported procedures. The solvents used were freshly distilled over the appropriate drying agent and used directly from the stills.

Synthesis of bis(diphenyldithiophosphinato)nickel(II), $[\text{Ni}((\text{C}_6\text{H}_5)_2\text{PS}_2)_2]$ (4**).** Complex **4** was synthesised and firstly X-ray characterised in 1968.¹¹ However, in this work we developed a new high yielding and clean synthetic route, which starts from primary phosphines: Ph_2PH (6.7 mL, 10%

water in hexane) was added to KCH_2Ph (0.3265 g, 2.5 mmol) in 10 mL of freshly distilled toluene at room temperature. After 10 minutes, the solution was transferred onto dried powdered S_8 (0.1588 g, 5 mmol), and the newly-formed brown suspension was transferred onto NiI_2 (0.3906 g, 1.25 mmol) and refluxed for 4 hours. The solvent was removed under reduced pressure and the resulting brown solid was dissolved in CH_2Cl_2 and filtered through a small celite plug. The filtrate was concentrated under vacuum and **4** obtained as purple crystals, suitable for X-ray analysis. $\text{C}_{24}\text{H}_{20}\text{P}_2\text{S}_4\text{Ni}$ (formula mass = 557.30 Da, 0.9971 g, 1.8 mmol, 72% yield). M.p.: 253–255 °C (m). ^1H NMR (400 MHz, D_6 -DMSO) δ = 7.22 (d, 3H, Ph), 7.94 (m, 2H, Ph); ^{31}P NMR (400 MHz, D_6 -DMSO) δ = 60.22.

Synthesis of $[\text{Ni}((\text{MeO})_2\text{PS}_2)\cdot\text{L1}]_\infty$, (1·L1**) $_\infty$.** Complex **1** (18.6 mg, 0.05 mmol) and **L1** (12.0 mg, 0.05 mmol) were reacted at 130 °C in a high pressure Aldrich tube in 30 mL of MeOH. After complete dissolving of the reagents, the reaction mixture was slowly cooled at room temperature. After a few days (**1·L1**) $_\infty$ (4.0 mg, 0.006 mmol, 13% yield) was obtained as green crystals suitable for X-ray analysis. M.p.: 170 °C (d). Elemental analysis found (calc. for $\text{C}_{16}\text{H}_{20}\text{N}_4\text{O}_4\text{P}_2\text{S}_5\text{Ni}$; formula mass = 611.9 Da): C, 31.63 (31.33); H, 2.38 (3.29); N, 9.31 (9.14); S, 21.75 (26.14). FT-IR (KBr, 3000–300 cm^{-1}): 2938 w, 2834 vw, 2361 vw, 1608 m, 1462 m, 1411 m, 1335 m, 1290 w, 1210 w, 1176 w, 1130 vs, 827 s, 798 s, 709 m, 691 s, 675 s, 665 m, 530 m, 439 vw, 398 w, 324 m cm^{-1} . FT-Raman (3500–100 cm^{-1} , 600 mW, solid state, relative intensities between parentheses related to the highest peak taken equal to 10.0): 1922 (6.0), 1894 (6.4), 1877 (6.0), 1811 (6.4), 1758 (4.6), 1612 (10.0), 1513 (8.6), 1459 (9.3), 1410 (9.3), 1335 (6.1), 1293 (6.0), 1020 (6.2) cm^{-1} .

Synthesis of $[\text{Ni}((\text{EtO})_2\text{PS}_2)\cdot\text{L1}]_\infty$, (2·L1**) $_\infty$.** Complex **2** (21.4 mg, 0.05 mmol) and **L1** (12.0 mg, 0.05 mmol) were reacted at 160 °C in a high pressure Aldrich tube in 30 mL of EtOH. After complete dissolving of the reagents, the reaction mixture was slowly cooled at room temperature. After a few days (**2·L1**) $_\infty$ (4.1 mg, 0.006 mmol, 12% yield) was obtained as green crystals suitable for X-ray analysis by slow evaporation of the solvent. M.p.: 155 °C (d). Elemental analysis found (calc. for $\text{C}_{20}\text{H}_{28}\text{N}_4\text{O}_4\text{P}_2\text{S}_5\text{Ni}$; formula mass = 668.0 Da): C, 36.31 (35.89); H, 4.17 (4.22); N, 8.46 (8.37); S, 24.12 (23.95). FT-IR (KBr, 3000–350 cm^{-1}): 3054 vw, 3032 w, 2934 w, 2893 vw, 2459 vw, 2285 vw, 1931 vw, 1609 s, 1496 vs, 1440 m, 1412 m, 1336 m, 1121 m, 1019 vs, 945 vs, 848 w, 830 m, 805 m, 773 s, 713 m, 673 s, 657 s, 644 m, 620 w, 546w, 410 w cm^{-1} . FT-Raman (3500–0 cm^{-1} , 150 mW, solid state, relative intensities between parentheses related to the highest peak taken equal to 10.0): 3075 (4.8), 3027 (4.2), 2933 (5.1), 2888 (5.0), 1981 (4.1), 1611 (10.0), 1513 (5.7), 1413 (8.5), 1338 (5.9), 1229 (5.3), 1215 (5.5), 1095 (7.7), 1015 (7.7) 999 (5.7), 729 (4.2), 650 (6.1) 548 (8.8), 376 (7.5) cm^{-1} .

Synthesis of $[\text{Ni}((\text{MeO})(4\text{-MeOC}_6\text{H}_4)\text{PS}_2)_2\cdot\text{L1}]_\infty$, (3·L1**) $_\infty$.** Complex **3** (26.2 mg, 0.05 mmol) and **L1** (12.0 mg, 0.05 mmol) were reacted at 100 °C in a high pressure Aldrich tube in 30 mL of CH_3OH . After complete dissolving of the reagents, the reaction mixture was slowly cooled at room temperature. After a week, (**3·L1**) $_\infty$ (29.5 mg, 0.39 mmol, 77% yield) was

obtained as green crystals suitable for X-ray analysis. M.p.: 160 °C (d). Elemental analysis found (calc. for $C_{28}H_{28}N_4O_4P_2S_5Ni$; formula mass = 764.0 Da): C, 44.73 (43.98); H, 3.38 (3.69); N, 7.53 (7.32); S, 21.08 (20.94). FT-IR (KBr, 1800-300): 1214 w, 1179 mw, 1130 vw, 1114 s, 1065 w, 1029 vs, 1020 vs, 909 vw, 851 vw, 830 ms, 779 vs, 754 w, 733 vw, 709 w, 690 vw, 654 ms, 640 s, 625 mw, 546 vs, 520 mw, 508 w, 457 vw, 442 w, 398 vw, 369 vw, 326 ms cm^{-1} . FT-Raman (3500-100 cm^{-1} , 150 mW, solid state, relative intensities between parentheses related to the highest peak taken equal to 10.0): 3054 (2.8), 2924 (2.8), 1615 (10.0), 1582 (5.7), 1420 (7.8), 1310 (3.6), 1280 (4.2), 1110 (5.7), 1020 (5.0), 1000 (5.0), 547 (6.4), 102 (6.4) cm^{-1} .

Synthesis of $[Ni((C_6H_5)_2PS_2)_2 \cdot L1]_{\infty}$, (4-L1) $_{\infty}$. A mixture of **4** (5.5 mg, 0.01 mmol) and **L1** (2.4 mg, 0.01 mmol) in 3 mL of toluene was heated to 100 °C in a sealed 5 mL screw-top glass bottle for 3 days. The mixture was allowed to cool to room temperature and the resulting green crystals of (4-L1) $_{\infty}$ filtered from the reaction mixture; (5.1 mg, 0.007 mmol, 64% yield) M.p.: >230 °C. Elemental analysis found (calc. for $C_{36}H_{28}N_4P_2S_5Ni$; formula mass = 797.57 Da): C, 44.88 (54.21); H, 3.45 (3.54); N, 4.93 (7.02)%. FT-IR (KBr, 4000-400 cm^{-1}): 3448 vw, 3045 w, 1607 s, 1465 s, 1435, 09 s, 1408 s, 1329 m, 1304 w, 1285 w, 1226 w, 1099 s, 1061 m, 999 m, 833 m, 823 m, 746 s, 707 vs, 699 vs, 612 vs, 571 s, 565 vs, 518 m, 483 m, 443 w, 420 w cm^{-1} .

Synthesis of $[Ni((MeO)_2PS_2)_2 \cdot L2]_2$, (1-L2) $_2$. Complex **1** (18.6 mg, 0.05 mmol) and **L2** (18.0 mg, 0.07 mmol) were reacted at 140 °C in a high pressure Aldrich tube in 30 mL of MeOH. After complete dissolving of the reagents, the reaction mixture was slowly cooled at room temperature. After a few days (1-L2) $_2$ (5.5 mg, 0.008 mmol, 18% yield) was obtained as green crystals suitable for X-ray analysis by slow evaporation of the solvent. M.p.: 180 °C (d). Elemental analysis found (calc. for $C_{16}H_{20}N_4O_4P_2S_5Ni$; formula mass = 611.9 Da): C, 31.55 (31.33); H, 2.21 (3.29); N, 9.13 (9.14); S, 24.69 (26.14). FT-IR (KBr, 4000-400 cm^{-1}): 2938 w, 2834 vw, 2361 vw, 1608 m, 1462 vm, 1411 m, 1335 m, 1290 w, 1210 w, 1176 w, 1130 vs, 827 s, 798 s, 709 m, 691 s, 675 s, 665 m, 530 m, 439 vw, 398 w, 324 m cm^{-1} . FT-Raman (4000-0 cm^{-1} , 200 mW, solid in KBr, relative intensities between parentheses related to the highest peak taken equal to 10.0): 1922 (6), 1894 (6.4), 1877 (6), 1811 (6.4), 1758 (4.6), 1612 (10), 1513 (8.6), 1459 (9.3), 1410 (9.3), 1335 (6.1), 1293 (6), 1020 (6.2) cm^{-1} .

Synthesis of $[Ni((EtO)_2PS_2)_2 \cdot L2]_2$, (2-L2) $_2$. A solution of **L2** (10 mg, 0.042 mmol) in 10 mL of EtOH was slowly diffused into a of CH_2Cl_2 solution of **2** (10 mg, 0.023 mmol, 0.5 mL) and left to stand at room temperature for several weeks. Green crystals of (2-L2) $_2$ (16.9 mg, 0.025 mmol, 50% yield) suitable for X-ray analysis were obtained. M.p.: 159-162 °C (m). Elemental analysis found (calc. for $C_{20}H_{28}N_4O_4P_2S_5Ni$; formula mass = 668.0 Da): C, 34.84 (35.89); H, 4.53 (4.22); N, 8.11 (8.37); S, 24.15 (23.95). FT-IR (KBr, 4000-50 cm^{-1}): 3054 vw, 3032 w, 2934 w, 2893 vw, 2459 vw, 2285 vw, 1931 vw, 1609 s, 1496 vs, 1440 m, 1412 m, 1336 m, 11215 m, 1019 vs, 945 vs, 848 w, 830 m, 805 m, 773 s, 713 m, 673 s, 657 s, 644 m, 620 w, 546 w, 410 w cm^{-1} . FT-Raman (3500-0 cm^{-1} , 600 mW, solid state, relative intensities between parentheses related to the highest

peak taken equal to 10.0): 3075 (4.8), 3027 (4.2), 2933 (5.1), 2888 (5), 1981 (4.1), 1611 (10), 1513 (5.7), 1413 (8.5), 1338 (5.9), 1229 (5.3), 1215 (5.5), 1095 (7.7), 1015 (7.7), 999 (5.7), 729 (4.2), 650 (6.1), 548 (8.8), 376 (7.5) cm^{-1} .

Synthesis of $[Ni((MeO)(4-MeOC_6H_4)PS_2)_2 \cdot L2]_{\infty}$, (3-L2) $_{\infty}$. Complex **3** (26.3 mg, 0.05 mmol) and **L2** (24.0 mg, 0.10 mmol) were reacted at 100 °C in a high pressure Aldrich tube in 25 mL of MeOH. After complete dissolving of the reagents, the reaction mixture was slowly cooled at room temperature. After a week, (3-L2) $_{\infty}$ (29.5 mg, 0.031 mmol, 62% yield) was obtained as green crystals suitable for X-ray analysis. M.p.: 160 °C (d). Elemental analysis found (calc. for $C_{28}H_{28}N_4O_4P_2S_5Ni$; formula mass = 764.0 uma): C, 44.73 (43.93); H, 3.38 (3.69); N, 7.53 (7.32); S, 21.08 (20.94). FT-IR (KBr, 1600-350 cm^{-1}): 1593 s, 1569 mw, 1499 s, 1474 ms, 1432 w, 1406 m, 1331 w, 1294 s, 1254 vs, 1175 ms, 1113 vs, 1021 vs, 827 mw, 775 vs, 730 w, 654 vs, 623 s, 545 vs, 525 w, 436 w, 406 vw, 327 ms cm^{-1} . FT-Raman (4000-0 cm^{-1} , 100 mW, solid in KBr, relative intensities between parentheses related to the highest peak taken equal to 10.0): 3054 (0.7), 2850 (0.4), 2670 (0.3), 1618 (5.2), 1477 (2.6), 1418 (2.0), 1199 (6.0), 1156 (10.0), 1031 (2.6), 642 (0.8), 545 (1.2), 125 (4.2), 104 (2.4) cm^{-1} .

Synthesis of $[Ni((C_6H_5)_2PS_2)_2 \cdot L2]_{\infty}$, (4-L2) $_{\infty}$. A mixture of **4** (5.5 mg, 0.01 mmol) and **L2** (2.4 mg, 0.01 mmol) in 3 mL toluene was heated to 100 °C in a sealed 5 mL screw-top glass bottle for 3 days. The mixture was allowed to cool to room temperature and the resulting green crystals filtered from the reaction mixture; (4.3 mg, 0.0042 mmol, 42% yield). M.p.: 233 °C (d). Elemental analysis found (calc. for $C_{48}H_{36}N_8P_2S_6Ni$; formula mass = 1037.86 Da): C, 54.2 (55.6); H, 3.5 (3.5); N, 10.8 (7.1)%. FT-IR (KBr, 4000-400 cm^{-1}): 3432 vw, 1637 w, 1587 m, 1497 s, 1471 vs, 1415 s, 1325 s, 1289 s, 1096 m, 1048 m, 1024 m, 998 m, 902 m, 815 s, 730 s, 693 s, 650 s, 611 m, 566 vs, 489 vs, 415 w cm^{-1} .

Characterisation

1H - and ^{31}P -NMR spectra were recorded at 25 °C in D_6 -DMSO on a Bruker DPX400 NMR spectrometer with internal standards. Elemental analyses were performed with an EA1108 CHNS-O Fisons instrument. FT-Infrared spectra were recorded on a Thermo Nicolet 5700 spectrometer at room temperature using a flow of dried air. Middle IR spectra (resolution 4 cm^{-1}) were recorded as KBr pellets, with a KBr beam-splitter and KBr windows. X-ray structure determinations and crystallographic data for compounds (1-L1) $_{\infty}$, (2-L1) $_{\infty}$, (3-L1) $_{\infty}$, (1-L2) $_2$, and (3-L2) $_{\infty}$, were collected at 120(2) K by means of combined phi and omega scans on a Bruker-Nonius Kappa CCD area detector, situated at the window of a FR591 rotating anode (graphite Mo- K_{α} radiation, λ = 0.71073 Å). Data for compound (2-L2) $_2$, were collected at 120(2) K by means of fine-slice/omega scans on Bruker SMART APEX2 CCD diffractometer with Daresbury SRS station 9.8 synchrotron source (silicon 111, λ = 0.6893 Å). Data for compound (4-L1) $_{\infty}$, were collected at 173(2) K by means of combined phi and diffractometer with enhance X-ray source

ARTICLE

Table 1 Selected bond lengths (Å), bond and torsion angles (°), and angles between pyridyl (Py)/thiadiazole (Tdz) ring mean planes (°) for (1-L1)_∞, (2-L1)_∞, (3-L1)_∞, and (4-L1)_∞. Numbering scheme according to Fig. S1.^b

	(1-L1) _∞	(2-L1) _∞	(3-L1) _∞	(4-L1) _∞
Ni–N1	2.095(3)	2.1042(16)	2.1343(18)	2.1376(16)
Ni–N4	2.100(3)	2.1042(16)	2.137(2)	2.1052(16)
Ni–S1	2.5041(12) ^a	2.4846(5)	2.4876(6) ^a	2.4836(5) ^a
Ni–S2	2.4585(11) ^a	2.4683(5)	2.4662(6) ^a	2.4940(6) ^a
P1–S1	1.9735(15) ^a	1.9693(8)	1.9993(9) ^a	2.0001(8) ^a
P1–S2	1.9814(15) ^a	1.9884(8)	1.9974(9) ^a	2.0025(7) ^a
N1–Ni–S1	91.02(8)	89.72(5)	90.94(5)	91.22(4)
N1–Ni–S2	89.58(9)	90.39(5)	89.12(5)	88.76(5)
S1–Ni–S2	82.04(4) ^a	82.010(17)	82.55(2) ^a	82.42(2) ^a
S1–P1–S2	110.95(7) ^a	110.39(3)	109.70(4) ^a	110.2(4) ^a
C2–C3–C6–N2	19(3)	31.9(3)	34.2(3)	4.7(3)
C9–C8–C7–N2	17(3)	31.9(3)	20.3(3)	11.0(3)
Py(N1)^Py(N4)	25.8	63.7	31.9	16.1
Py(N1)^Tdz	20.1	32.9	36.5	4.9
Py(N4)^Tdz	17.3	32.9	20.0	11.4

^a Average of the bond parameters for the two symmetry independent fragments (P₁S₁S₂Ni₁) and (P₂S₁S₂Ni₂). Due to the different space groups own by the polymers, as a consequence, to the different equivalent atoms imposed by symmetry, each structure had to be solved with different labels. In order to compare structural parameters of differently labelled polymers, Table 1 refers to the common artificial numbering scheme shown in Fig. S1.

(graphite Mo-K_α radiation). Data for compound (4-L2·2C₇H₈)_∞, were collected at 173(2) K by means of omega scans on an Oxford Diffraction Xcalibur PX Ultra diffractometer with enhance ultra (Cu) X-ray source (graphite Cu-K_α radiation, λ = 1.54184 Å). The structures were solved by direct methods, SHELXS-97 and refined on F² using SHELXL-97.^{12,13} Anisotropic displacement parameters were assigned to all non-hydrogen atoms. Hydrogen atoms were included in the refinement, but thermal parameters and geometry were constrained to ride on the atom to which they are bonded. The data of (1-L1)_∞, (2-L1)_∞ and (3-L1)_∞ were corrected for absorption effects using SADABS V2.10.¹⁴ The data for (4-L1)_∞ and (4-L2)_∞ were refined using CrysAlis RED,¹⁵ implemented in SCALE3 ABSPACK scaling algorithm for empirical absorption correction using spherical harmonics. Structures have been deposited with the Cambridge Crystallographic Data Centre: deposition numbers

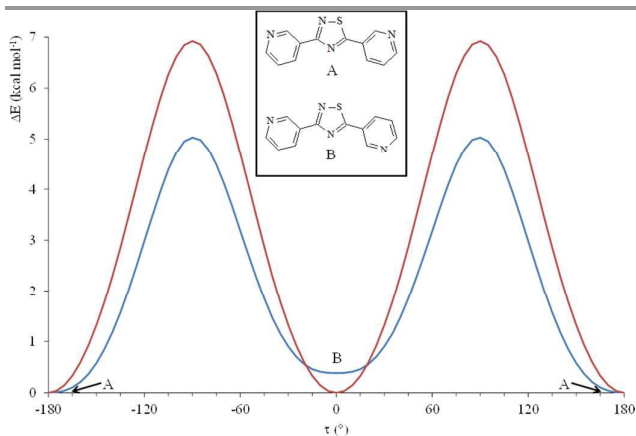


Fig. 1 Relative electronic energy variation ΔE as a function of the rotation angle τ of one pyridine ring (rotation step 5.0°) calculated at DFT level for L1 (red) and L2 (blue). In the inset the two possible *cisoid*s (A) and *transoid* (B) L2 conformers are depicted. $\Delta E_B - \Delta E_A = 0.39$ kcal mol⁻¹.

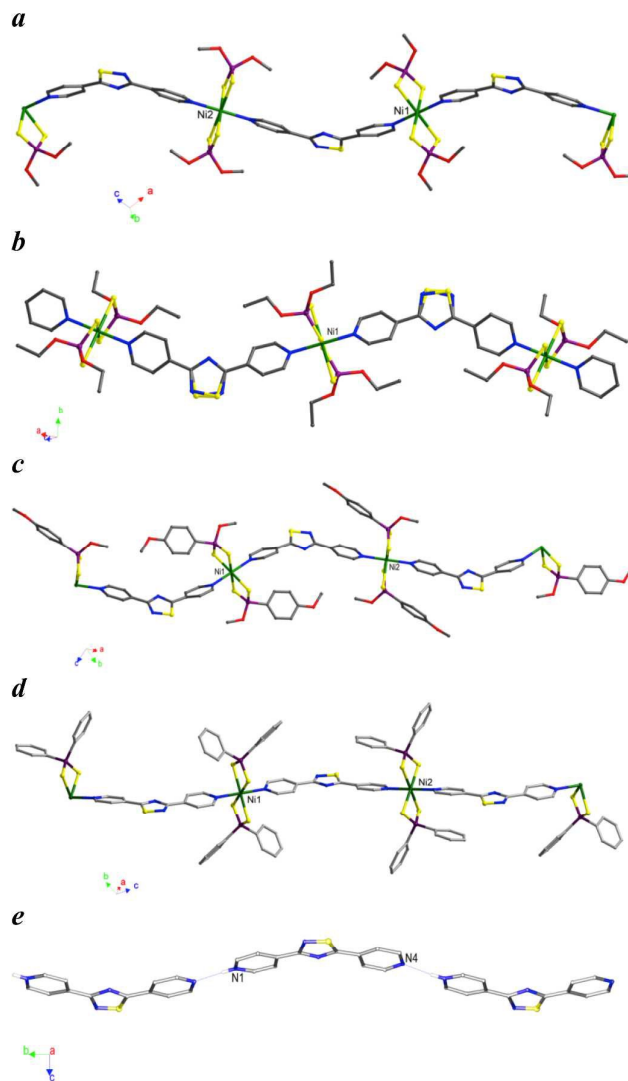


Fig. 2 Polymeric and protonated chains involving ligand L1 in the compounds (1-L1)_∞ (a), (2-L1)_∞ (b), (3-L1)_∞ (c), (4-L1)_∞ (d), and (L1H⁺)_∞ (e; ref. 10).

CCDC 1474147, 1474143, 1474148, 1474145, 1474150, 1474144, 1474146, and 1474149, for (1-L1)_∞, (2-L1)_∞, (3-L1)_∞, (4-L1)_∞, (1-L2)₂, (2-L2)₂, (3-L2)_∞, and (4-L2·2C₇H₈)_∞, respectively. Theoretical calculations based on Density Functional Theory (DFT)¹⁶ were carried out on L1 and L2 with the Gaussian09¹⁷ commercial suite of software by adopting the mPW1PW¹⁸ functional and Schäfer, Horn, and Ahlrichs double-zeta plus polarisation (pVDZ) all-electron basis sets (BSs) for all atomic species.¹⁹ A potential energy surface was carried out by rotating by an angle τ one of the pyridine rings ($-180.0^\circ \leq \tau \leq 180.0^\circ$; $\Delta\tau = 5.0^\circ$). The programmes GaussView 5.0.8 and Molden 5.2 were used to investigate the charge distributions and MO shapes.²⁰

Results

The *bis*-functional ligands L1 and L2 (Scheme 1) were first isolated by Meltzer *et al.* in 1955,²¹ but their complexing ability

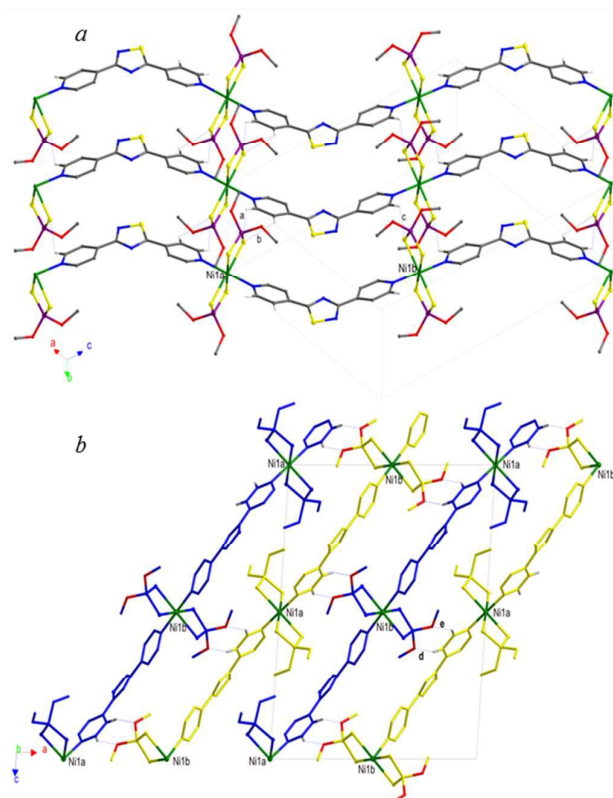


Fig. 3 Packing view of $(1-L1)_\infty$ showing parallel chains interacting through C-H...S interactions (a; H...S distances and C-H...S angles: a, C9-H9...S2 2.89(3), 120(2); b, C8-H8...S5 2.85(3), 122(2); c, C15-H15...S3 2.91(4) Å, 126(2)°; $x, -1+y, z$); (b) view along the 010 direction with polymeric chains coloured in blue and yellow according to their orientation. The Ni^{II} ions and the O and H atoms involved in the described H-bonds (d, C6-H6...O3 2.37(4), 3.288(5), 155(3); e, C5-H5...O4 2.60(4) Å, 3.419(5) Å, 148(3)°; $x, 1.5-y, 0.5+z$) have been left of the conventional colours.

towards metal ions, or as Lewis donors, has not been investigated to date. In fact, a search in the Cambridge Crystallographic Data Base revealed only a recent work by Ondrejovicova et al.²² Both **L1** and **L2** contain two pyridyl groups linked by a 1,2,4-thiadiazole ring acting as a rigid, non-reactive spacer. Compared with the popular 4,4'-bipyridine linker, the pyridyl rings in **L1** and **L2** feature different geometry and separation lengths (9.95 and 9.60 Å, respectively). Moreover, due to the different position of the nitrogen atoms in **L1** and **L2** and to the different rotational conformations possible for the pyridyl rings, several orientations of the binding sites can be expected. A Potential Energy Surface (PES) analysis carried out on **L1** and **L2** at DFT level in the gas phase by rotating one pyridyl substituent by an angle τ ranging between -180 and 180° clearly shows that both donors display an energy minimum when the central 1,2,4-thiadiazole ring is coplanar with the pyridine moieties (Fig. 1). In the case of **L2**, two planar isomers, *cisoid* and *transoid*, are possible, differing in energy by less than 1 kcal mol⁻¹ and showing similar metric parameters. As previously described, **L1** and **L2** feature the highest Kohn-Sham molecular orbitals localized on the negatively charged nitrogen atoms of the two pyridine moieties, which are therefore available to behave as donor sites towards Lewis unsaturated metal complexes.¹⁰ The reactions of **L1** with nickel dithiophosphato $[Ni((RO)_2PS_2)_2]$ [R =

Me (**1**), Et (**2**); Scheme 1]; dithiophosphonato $[Ni(MeOdtpp)_2]$ (**3**) [$MeOdtpp = (CH_3O)(4-MeOC_6H_4)PS_2^-$, Scheme 1], and dithiophosphito $[Ni(Ph_2PS_2)_2]$ (**4**) complexes under solvothermal conditions afforded solid, crystalline compounds, which were isolated and identified by means of single crystal X-ray diffraction as coordination polymers of formula $(1-L1)_\infty$, $(2-L1)_\infty$, $(3-L1)_\infty$, and $(4-L1)_\infty$, respectively. Crystallographic data and selected bond lengths and angles are reported in Tables S1 and 1 respectively. With the exception of compound $(4-L1)_\infty$, the **L1** molecules are found in two different but essentially superimposable orientations, arising from a 180° rotation of the molecule about the direction passing through the midpoint of the N-S bond and through the remaining nitrogen atom of the penta-atomic ring (Figs. S1–S3). As a consequence, the nitrogen and the adjacent sulfur atoms show fractional occupancies refined at values of about 60% and 40%, respectively, and only the major orientation of the molecule is illustrated in the figures. In the case of compound $(2-L1)_\infty$ the **L1** molecule is located about a crystallographic two-fold axis and therefore the resulting disorder is modelled with occupancies of 50% for each orientation.

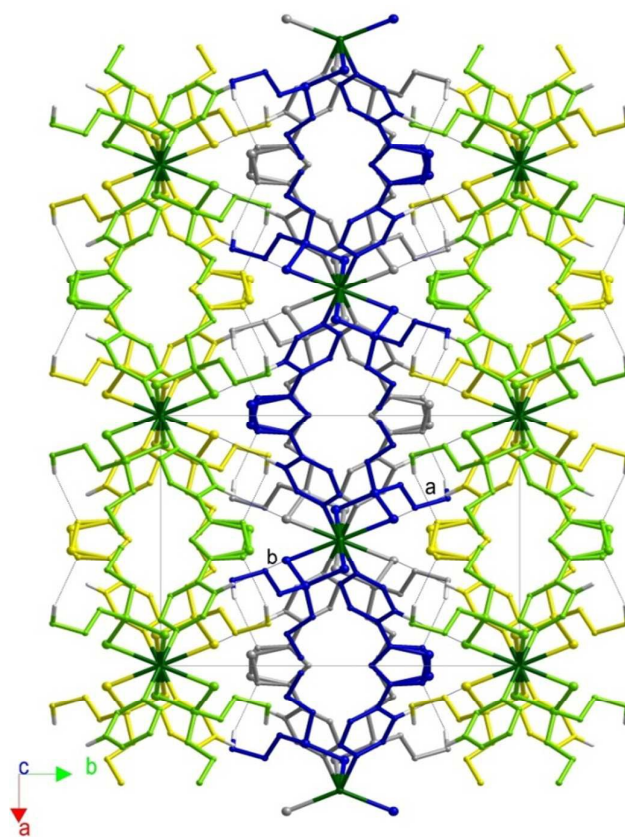


Fig. 4 Packing view along the 001 direction of $(2-L1)_\infty$ showing polymeric chains differently coloured according to their orientation. The Ni^{II} ions and the H atoms involved in the described H-bonds [a, C2-H2a...N3/S3ⁱ 2.54(4)/2.73(3), 3.426(10)/3.617(5), 147(2)/148(2); C5-H5...S2ⁱⁱ 2.85(2) Å, 3.364(2) Å, 115(2)°; $x, -y, 0.5+z$; $^i -0.5+x, 0.5-y, 1-z$] have been left of the conventional colours. H-atoms not involved in showed interactions have been omitted for clarity. The labels used for the described interactions refer to the original numbering scheme (Fig. S2).

Coordination polymers $(1-4-L1)_\infty$ show similar coordination environments: the nickel ions display distorted octahedral geometries with the equatorial plane occupied in iso-bidentate bonds with two dithiophosphoric ligands and the pyridine rings belonging to spacer **L1** axially bridging adjacent Ni^{II} ions to form infinite polymeric chains. The relevant bond lengths and angles (Table 1) are similar to those found in analogous coordination polymers.^{7,8,9} The structures of the coordination polymers share the presence of neutral undulated polymeric chains with very similar pitches: Ni-Ni distances, through coordinate bonds, of 13.70, 14.15, 13.97, and 14.02 Å for $(1-L1)_\infty$, $(2-L1)_\infty$, $(3-L1)_\infty$, and $(4-L1)_\infty$, respectively (Fig. 2). These chains are closely analogous to the $C_1^1(12)$ chains of type $[...(\text{Py}\cap\text{PyH}^+\cdots\text{Py}\cap\text{PyH}^+)\cdots]$ built up through the moderate $\text{NH}\cdots\text{N}$ bonds derived by the protonation of **L1** molecules, reported for comparison in Fig. 2e.¹⁰ This confirms that the orientation of the nitrogen atoms *para*-positioned in the outwards pyridyl rings of **L1** self-govern the geometry of the resulting supramolecular aggregates, leading to similar shapes independent of the nature of the interacting Lewis acid. The asymmetric unit of compound $(1-L1)_\infty$ (Fig. S2, Fig. 2a) contains two independent Ni^{II} ions, namely Ni1 and Ni2, lying on crystallographic inversion centres with coordination sites differing in the orientation of the methoxy substituents at the phosphorous atoms. The two coordination sites are bridged by **L1** molecules thus forming 1D parallel chains propagating along the 101 direction. These chains interact to each other through C-H \cdots S short contacts, involving the pyridine rings and the coordinated sulphur atoms, leading to the 2D layers shown in Fig. 3a. The polymeric chains pack in two different orientations (coloured blue and yellow in Fig. 3b and S3) generated by inversion along the screw axes parallel to the 010 direction. As a consequence, symmetry related 2D layers formed by differently oriented chains alternate when packed and interact through synergic C-H \cdots O bonds ("d" and "e" in Fig. 3b and S3a) involving the pyridine rings and the methoxy P-substituents belonging to Ni1b coordination sphere in a $R_2^2(7)$ motif. This packing arrangement enables the formation of "rippled" void channels of about 60 Å³ corresponding to 2.2% of the unit cell volume (Fig. S3b). The presence of OEt P-substituents in place of the OMe ones in the compound $(2-L1)_\infty$ (Fig. 2b, Fig. S4) does not result in significant changes in either the Ni^{II} coordination environment or in the primary motif of the polymer and no relevant intramolecular interactions are worthy of note. The polymeric chains assume four symmetry related orientations as illustrated in the colour scheme in Fig. 4. Pairs of symmetry related chains propagating

in the $[10(1/2)]$ (yellow and green in Fig. 4) and $[-10(1/2)]$ (blue and grey in Fig. 4) directions, respectively, interact through weak H-bonds involving the P-substituents and the central thiadiazole ring of **L1** ("a" in Fig. 4) form 2D layers which stack along the $[010]$ direction leading to a very dense packing with no voids.

The coordination polymers $(3-L1)_\infty$ and $(4-L1)_\infty$ (Figs. 2c, 2d, S5 and S6) are characterised by the presence of aryl substituents at the phosphorous atoms which are expected to engender additional *intra*- and *inter*-molecular aromatic interactions. Similarly to those described previously herein, the asymmetric units of compounds $(3-L1)_\infty$ and $(4-L1)_\infty$ contain two independent Ni^{II} ions located on crystallographic inversion centres and differing only in the orientation of the aryl P-substituents. In the coordination polymer $(3-L1)_\infty$ the interactions involving the aromatic rings are intramolecular in nature (edge-to-face interaction "a" in Fig. 5). Weak interactions between the methoxy groups (interactions "b" and "c" in Fig. 5) connect the chains in layers which pack parallel to each other, forming a three-dimensional network through C-H \cdots S interactions mainly involving the coordinated sulphur atoms and the methoxy substituents (interactions "d"- "g" in Fig. 5Sb).

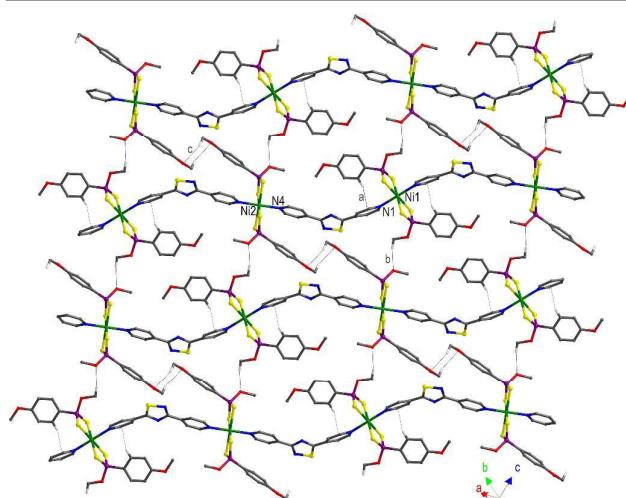


Fig. 5 Packing views of $(3-L1)_\infty$ showing layers of undulated chains; a, C2-H2 \cdots CntPy(N1) 2.62 Å; b, C8-H8c \cdots O3ⁱ 2.24, 3.171(3), 158.0; c, C15-H15a \cdots O4ⁱⁱ 2.53 Å, 3.237(3) Å, 129.0°; ⁱ $-1+x, -1+y, z$; ⁱⁱ $2-x, 2-y, -z$. H-atoms not involved in showed interactions have been omitted for clarity. The labels used for the described interactions refer to the original numbering scheme (Fig. S5).

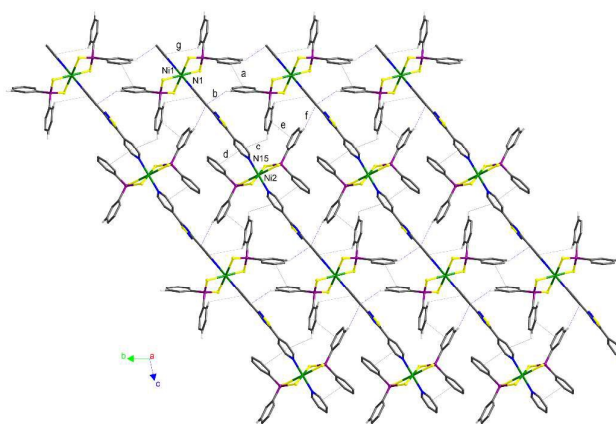
Table 2 Selected bond lengths (Å), bond and torsion angles (°), and angles between pyridyl (Py)/thiadiazole (TdZ) ring mean planes (°) for (1-L2)₂, (2-L2)₂, (3-L2)_∞, and (4-L2·2C₇H₈)_∞. Numbering scheme according to Fig. S7.

	(1-L2) ₂	(2-L2) ₂	(3-L2) _∞	(4-L2)·2C ₇ H ₈) _∞
Ni–N1	2.093(5)	2.103(5) ^b	2.160(2)	2.129(6)
Ni–N4	2.099(5)	2.100(5) ^b	2.160(2)	2.129(6)
Ni–S1	2.4928(18) ^a	2.500(2) ^b	2.4915(6)	2.4809(15)
Ni–S2	2.4846(18) ^a	2.487(2) ^b	2.4871(6)	2.4995(17)
P1–S1	1.979(2) ^a	1.969(3) ^b	1.9974(8)	2.0059(19)
P1–S2	1.981(2) ^a	1.976(3) ^b	1.9915(9)	1.997(2)
N1–Ni–S1	90.66(15)	89.93(19) ^b	88.91(5)	90.82(11)
N1–Ni–S2	88.99(15)	89.76(18) ^b	90.52(5)	89.35(11)
S1–Ni–S2	81.89(10) ^a	81.98(8) ^b	81.86(2)	83.00(5)
S1–P1–S2	110.93(10) ^a	112.0(2) ^b	109.71(4)	111.08(8)
N1–Ni–N4	175.7(2)	176.3(2) ^b	180.00	180.00
N2–C6–C3–C2	9.6(3)	1.4(11) ^b	11.7(3)	0.0
N2–C7–C8–C9	17.9(3)	4.4(11) ^b	11.7(3)	0.0
Py(N1)^Py(N4)	12.3	5.0 ^b	19.2	0.0
Py(N1)^TdZ	4.3	3.0 ^b	14.7	0.0
Py(N4)^TdZ	20.3	7.2 ^b	14.7	0.0

^a Average of the bond parameters for the two fragments (P₂S₂Ni) and (P₂S₂Ni). ^b Average of the bond parameters for the symmetry independent coordination environment around Ni1 and Ni2.

Aromatic interactions become prevalent in polymer (4-L1)_∞ due to the presence of phenyl substituents at the phosphorous atoms, so that the polymeric chains pack in layers built up by face-to-face and edge-to-face interactions only ("a"–"g" in Fig. 6). The layers pack parallel to the *a* axis through weak C–H...S interactions ("h"–"j" in Fig. 6Sb). Despite the fact that all the coordination polymers featuring L1 as a spacer exhibit the same primary motif found in the supramolecular aggregates of L1H⁺ (Fig. 2e), the presence and orientation of the P-substituents influences the final architecture of the polymers via aromatic or C–H...S intramolecular interactions. The main consequence is the loss of planarity of the bridging L1 ligands (Table 1), probably ascribable to the conformational arrangement the pyridine rings adopt to optimize these interactions. It is interesting to note that in the H-bonded chains built up by protonated L1 molecules, where such interactions are not present, the ligands retain planarity.¹⁰

The reactions of L2 with the nickel complexes 1–4 under solvothermal conditions afforded crystalline compounds recognised by means of single crystal X-ray diffraction as the dimers (1-L2)₂, (2-L2)₂, and the coordination polymers (3-L2)_∞, and (4-L2)_∞ in the compound (4-L2·2C₇H₈)_∞, respectively (Figs. 7–10, S8–S11). The two different constructs reflect the different conformations of L2 behaving as a convergent linker in the dimeric structures and as divergent linker in the polymers. Crystallographic data and selected bond lengths and angles are reported in Tables S2 and 2. Similarly to the previously discussed cases of polymers (1–3-L1)_∞, in the crystal structures of the dimer (1-L2)₂ and the polymers (3–4-L2)_∞ the spacer L2 is located in two essentially superimposable orientations. As a consequence, the nitrogen and the adjacent sulfur atoms show fractional occupancies refined at values of 68.8 and 31.2% for (1-L2)₂, and 61.5 and 31.5% for (4-L2)_∞ (the figures represent the molecules in the major orientation only).

**Fig. 6** Packing view of (4-L1)_∞ showing layers built up by the aromatic interactions a–g: a, Cnt_{PH}(C24–C29)···Cnt_{PH}(C24–C29)ⁱ 4.16, 0; b, Cnt_{Py}(N1)···H26–C26ⁱ 3.32, 49; c, Cnt_{Py}(N15)ⁱ···H21aⁱ–C21ⁱ 3.08, 133; d, Cnt_{Py}(N15)ⁱ···Cnt_{PH}(C36–C41) 3.67, 11; e, Cnt_{PH}(C30–C35)ⁱ···Cnt_{PH}(C18–C23) 3.90, 19; f, C34–H34a···Cnt_{Py}(N1) 3.58, 109; g, C19^{iv}–H19a^{iv}···Cnt_{Py}(N1) 3.90 Å, 129°. Symmetry codes: ⁱ –*x*, 1–*y*, 1–*z*; ⁱⁱ 1–*x*, 1–*y*, 2–*z*; ⁱⁱⁱ *x*, –1+*y*, *z*; ^{iv} –*x*, 2–*y*, –*z*. H-atoms not involved in showed interactions have been omitted for clarity. The labels used for the described interactions refer to the original numbering scheme (Fig. S6).

In the case of compound (3-L2)_∞ the L2 molecule is located about a crystallographic two-fold axis and therefore the resulting disorder is modelled with occupancies of 50% for each orientation. The asymmetric unit of the dimer (2-L2)₂ contains two independent units featuring differently oriented ligands L2 (Fig. 7b). Both dimers (1–2-L2)₂ and polymers (3–4-L2)_∞ display octahedral Ni^{II} coordination environments similar to those previously discussed, with two iso-bidentate dithiophosphoric ligands in the equatorial plane and the axial positions occupied by the pyridine rings of L2 bridging spacers. The bond lengths and angles (Table 2) are also similar to those found in the analogous coordination polymers (1–4-L1)_∞. Notwithstanding similarities with the results obtained with L1, the use of L2 as a linker leads to different constructs. In fact, as evidenced by DFT calculations (see above), L2 can exist either as a *transoid* or *cisoids* isomer and a convergent or a divergent conformation can be distinguished depending on the orientation of N-atoms of the pyridyl rings that can point inwards or outwards with respect to the pinch angle. In (1-L2)₂ and (2-L2)₂ the pyridyl rings of ligand L2 are oriented in a convergent fashion leading to closed rings rather than polymeric chains (Fig. 7a–b). It is interesting to note that this construct is far from predictable in its behaviour since a convergent fashion does not necessarily lead to closed rings. This is demonstrated by the formation of the mono-dimensional C₁¹(10) spirals found in the two structures of (HL2)₁ and (HL2)₁ assembled through NH⁺···N bonds between protonated L2 molecules exhibiting a convergent *cisoids* conformation.¹⁰ In dimers (1-L2)₂ and (2-L2)₂ two spacers bridge two dithiophosphato nickel complexes through axial coordination generating eicos-atomic planar wheels with openings of about 8 × 8 Å², and inner Ni···Ni distances of 7.73, 7.77, and 7.58 Å for (1-L2)₂ and the two independent units of (2-L2)₂, respectively.

ARTICLE

Journal Name

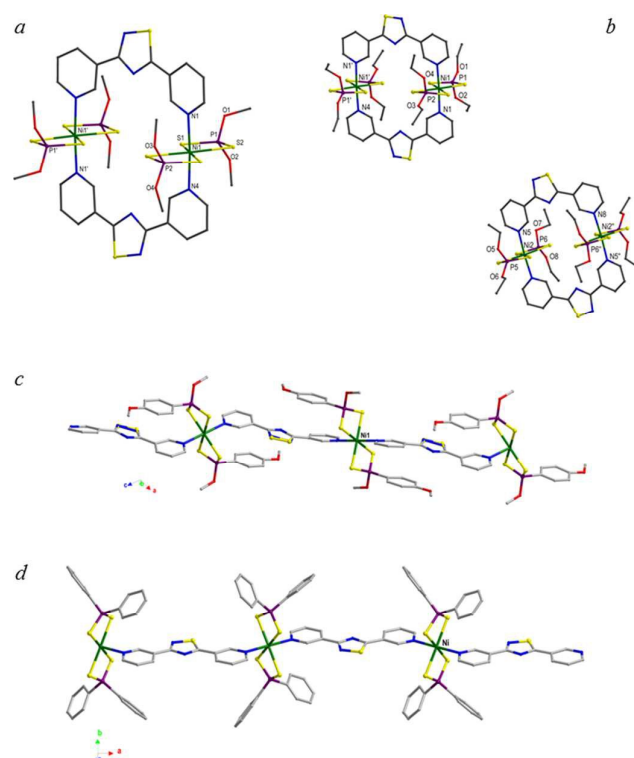


Fig. 7 Dimeric units and polymeric chains for (1-L2)₂ (a), (2-L2)₂ (b), (3-L2)_∞ (c), and (4-L2)_∞ in compound (4-L2·2C₇H₈)_∞ (d). The labels reported refer to the original numbering schemes (Figs. S8–S12). H-atoms have been omitted for clarity. Only the labels used in the discussion are here reported.

Despite the analogies in their structures, the dimers (1-L2)₂ and (2-L2)₂ show different packing arrangements. The dimers (1-L2)₂ are arrayed in regular perforated layers assembled by N[⋯]H and S[⋯]H interactions (Fig. 8a). Symmetry related parallel layers pack in an off-set compact arrangement along the *b* direction showed in Fig. 8.

In the crystal packing of (2-L2)₂ the two symmetrical independent units (containing Ni^{II} and Ni^{II} ions) that, as previously observed differ in the orientation of the thiadiazole ring (Td_z), interact with each other through π–π interactions involving the pyridine and Td_z rings forming puckered ribbons (Fig. 9a). A view along the *a* axis (Fig. 9b) shows the ribbons aligned in a parallel arrangement through H-bonds and weaker interactions mainly involving the sulphur atoms and the pyridine hydrogens. A *cisoid* but divergent conformation of L2 leads to the coordination polymers (3-L2)_∞ and (4-L2)_∞ (Figs. 7c–d, S10–S12). The asymmetric units of both compounds contain one independent Ni^{II} ion situated on a crystallographic inversion centre in the first case and on a mirror plane in the latter. The polymeric supramolecular constructs present close analogies with the C₁¹(10) chains formed by head-to-tail NH⁺⋯N bonds between adjacent pyridine rings of protonated L2 molecules featuring a *trans* conformation.¹⁰ Both complexes 3 and 4 feature aromatic substituents that are involved in π-type interactions which govern the assembly of the relevant polymers. In (3-L2)_∞ the aromatic P-substituents engage in intramolecular π–π interactions with the facing pyridine rings

and intermolecular C–H⋯O interactions with the oxygen belonging to the MeO P-substituents which connect the chains in layers (interactions a and b in Fig. S12a). The layers pack in parallel through C–H⋯S interactions involving the *para*-methoxy group of the Ar–P substituents and the coordinated sulphur atoms (interactions c–e in Fig. S12b), thus forming an overall three-dimensional network. Solvent accessible voids of 69 Å³ (in blue in the inset of Fig. S12), correspond to 4% of the unit cell volume. In polymer (4-L2)_∞ the exclusive presence of phenyl substituents at the phosphorous atoms results in the aromatic interactions becoming prevalent such that the parallel polymeric chains pack through edge-to-face interactions only (Fig. 10a). The resulting network features empty channels suitable for the inclusion of toluene molecules which engage in π-interactions with the phenyl rings (Fig. 10b–c). It is interesting to note that, in contrast to the previously discussed structures (see also Tables 1 and 2), (4-L2)_∞ contains perfectly planar L2 ligands.

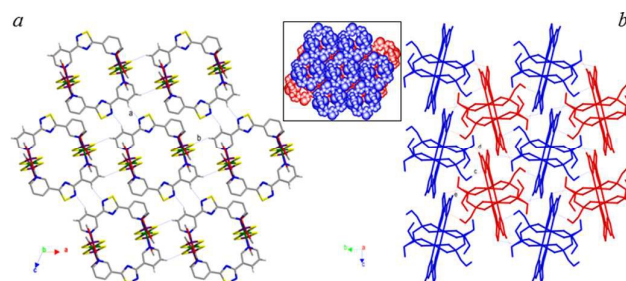


Fig. 8 Packing views showing the (a) layers formed by interacting (1-L2)₂ dimers and (b) packing of intercalating layers evidenced in different colours; in the inset the intercalating layers packing along the 010 direction are presented. All the hydrogen atoms with the exception of those involved in the showed interactions have been omitted. Interactions: a: C14i–H14ⁱ⋯N3, 2.70(9), 3.331(13), 124; b: C15ⁱⁱ–H15ⁱⁱ⋯S2, 2.93(9), 3.618(8), 127; c: C1ⁱⁱⁱ–H1bⁱⁱⁱ⋯N2, 2.57, 3.365(19), 138; d: C2ⁱⁱⁱ–H2aⁱⁱⁱ⋯S5, 2.88, 3.542(8), 126; e: C8^{iv}–H8^{iv}⋯O3, 2.59 Å, 3.504(9) Å, 161°. Symmetry codes: ⁱ –1+x, y, –1+z; ⁱⁱ 1–x, 1–y, 1–z; ⁱⁱⁱ –x, 0.5+y, 0.5–z; ^{iv} x, 1.5–y, 0.5+z.

Conclusions

The reaction of L1 with the differently P-substituted dithiophosphonato, dithiophosphato, and dithiophosphito complexes 1–4 yielded the corresponding coordination polymers (1–4-L1)_∞ featuring polymeric assemblies [⋯(Py⋯PyH⁺⋯Py⋯PyH⁺)_n⋯] built up through the moderate NH⁺⋯N bonds derived by the protonation of L1 molecules. These results indicate that L1 can be used as a spacer for the predictable assembly of smoothly undulating chains independent of the nature of the interacting Lewis acid, since the orientation of the nitrogen atoms *para*-positioned in the outwards pyridyl rings of L1 self-governs the geometry of the resulting supramolecular construct. On the contrary, L2 allows for the existence of different supramolecular constructs ensuing from different ligand conformations deriving from the rotation of the pyridyl rings.

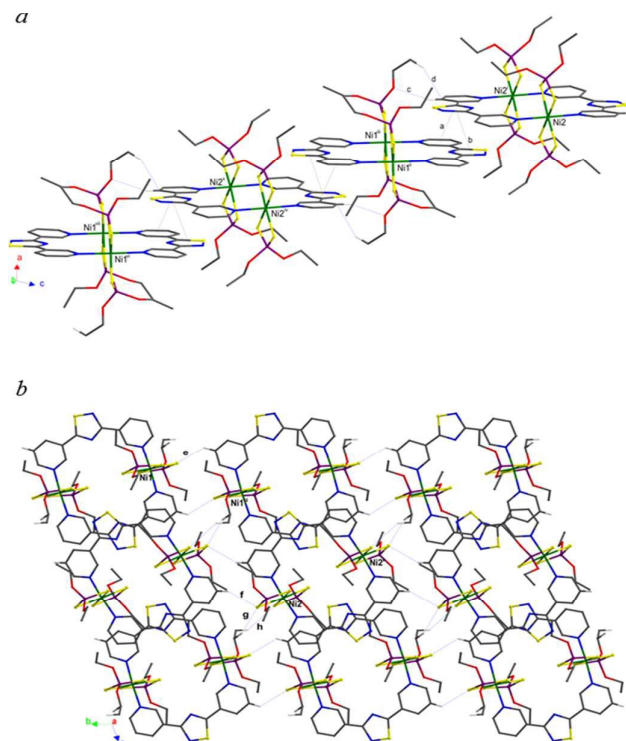


Fig. 9 Packing views showing (a) the ribbons formed by π - π interacting (2-L2)₂ dimers and (b) packing view along 100 direction of interacting ribbons. All the hydrogen atoms with the exception of those involved in the showed interactions have been omitted. Shown π - π interactions (a, b), weak contacts (c, d, e, g, h), and the H-bond (f): a, Cnt_{py(N8)}...Cnt_{py(N1)} 3.58, Py(N5)⁺Py(N4)⁺ 1; b, Cnt_{py(N15)}...Cnt_{py(N15)} 3.44 Å, Tdz_(S15)...Tdz_(S5) 1; c, C38-H38...O3ⁱⁱⁱ 2.40 Å; d, C6ⁱⁱⁱ-H6^c...C38, 2.78; e, C12ⁱⁱ-H12ⁱⁱ...S2, 2.89; g, C1^{ix}-H1a^{ix}...S12, 2.99; h, C2^{ix}-H2a^{ix}...S13, 3.04 Å; f, C32ⁱⁱⁱ-H32ⁱⁱⁱ...S12, 2.77 Å, 3.596(9) Å, 146°. Symmetry codes: 2-x, -y, 1-z; 1-x, 1-y, -z; 1-x, -1+y, -1+z; 2-x, 1-y, 1-z; 1+x, y, 1+z.

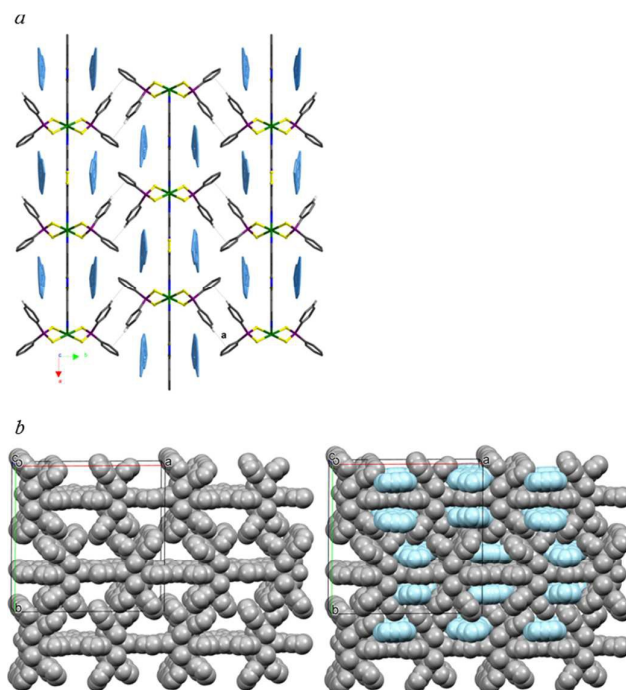


Fig. 10 (a) Packing view along the 001 direction of the parallel chains of (4-L2)_∞ with the toluene molecules included in the crystal evidenced in light blue colour. All the hydrogen atoms have been omitted with the exception of those involved in the showed interaction a, C27-H27a...Cnt_{py(N18-C23)} 2.84 Å, (Ph_(C24-C29)^ (Ph_(C18-C23)) 91.4°. Symmetry code: 1.5-x, 1-y, 0.5+z. (b) Space-fill view of the network with (left) and without (right) the solvent molecules.

In particular, the results suggest that aromatic P-substituents capable of π -interacting with the aromatic rings of the ligand tend to favour divergent constructs. The influence of secondary interactions involving the P-substituents is confirmed by the loss of planarity of **L1** and **L2** in order to enhance inter-molecular packing interactions.

Acknowledgements

MCA, MA, FI and VL kindly acknowledge the Dipartimento di Scienze Chimiche e Geologiche of the Università degli Studi di Cagliari and Banco di Sardegna for financial support (PRID 2015).

Notes and references

† The 112 issue of *Chem. Rev.* (2012) and the 16 issue of *Chem. Soc. Rev.* (2014) were entirely devoted to the synthesis and applications of MOF's showing how rapidly this branch of solid state materials chemistry is being evolving.

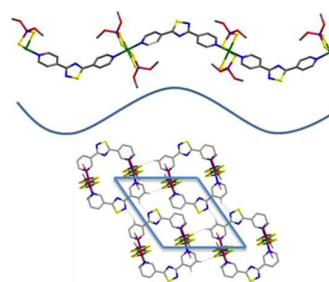
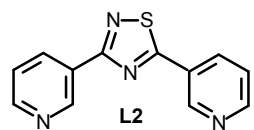
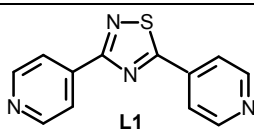
§ Among the ligands most commonly employed as spacers the choice of using 4,4'-bipyridine and its analogues is due to their versatility. In fact, by introducing different groups between the two pyridyl rings a wide variety of either linear or bent, rigid or flexible spacers are available. See for example ref. 4.

- 1 Y. Wang, B. Yuan, Y.-Y. Xu, X.-G. Wang, B. Ding and X.-J. Zhao, *Chem. – Eur. J.* 2015, **21**, 2107-2116; X. Zhang, W. Wang, Z. Hu, G. Wang and K. Uvdal, *Coord. Chem. Rev.*, 2015, **284**, 206-235; P. Ramaswamy, N. E. Wong and G. K. H. Shimizu, *Chem. Soc. Rev.*, 2014, **43**, 5913-5932; A.M. Fracaro, H. Furukawa, M. Suzuki, M. Dodd, S. Okajima, F. Gándara, J.A. Reimer and O.M. Yaghi, *J. Am. Chem. Soc.*, 2014, **136**, 8863-8866; J. Liu, L. Chen, H. Cui, J. Zhang, L. Zhang and C. Su, *Chem. Soc. Rev.*, 2014, **43**, 6011-6061; V. Stavila, A. A. Talin and M. D. Allendorf, *Chem. Soc. Rev.*, 2014, **43**, 5994-6010. P. R. Ashton, V. Balzani, A. Credi, O. Kocian, D. Pasini, L. Prodi, N. Spencer, J. F. Stoddart, M. S. Tolley, M. Venturi, A. J. P. White and D. J. Williams, *Chem. Eur. J.*, 1998, **4**, 590-607.
- 2 W. Lu, Z. Wei, Z.-Y. Gu, T.-F. Liu, J. Park, J. Park, J. Tian, M. Zhang, Q. Zhang, T. Gentle III, M. Bosch and H.-C. Zhou,

- Chem. Soc. Rev.*, 2014, **43**, 5561-5593; M. C. Aragoni, M. Arca, F. A. Devillanova, M. B. Hursthouse, S. L. Huth, F. Isaia, V. Lippolis, A. Mancini, S. Soddu and G. Verani, *Dalton Trans.* 2007, 2127-2134; A.-L. Cheng, N. L. Yan-Feng Yue, Y.-W. Jiang, E.-Q. Gao, C.-H. Yan and M.-Y. He, *Chem. Commun.*, 2007, 407-409; Z.-F. Chen, S.-F. Zhang, H.-S. Luo, B. F. Abrahams and H. Liang, *CrystEngComm*, 2007, **9**, 27-29; K. Biradha, M. Sarkar and L. Rajput, *Chem. Commun.*, 2006, 4169-4179; I. Goldberg, *Chem. Commun.*, 2005, 1243-1254; D. Braga, L. Brammer and N. R. Champness, *CrystEngComm*, 2005, **7**, 1-19; L. Brammer, *Chem. Soc. Rev.*, 2004, **33**, 476-489; S. Kitagawa, R. Kitaura and S.-I. Noro, *Angew. Chem., Int. Ed.*, 2004, **43**, 2334-2375; C. B. Aakeröy, J. Desper and J. Valdés-Martínez, *CrystEngComm*, 2004, **6**, 413-418; B. Rather and M. J. Zaworotko, *Chem. Commun.*, 2003, 830-831; E.-Q. Gao, S.-Q. Bai, Z.-M. Wanga and C.-H. Yan *Dalton Trans.*, 2003, 1759-1764; S. Sain, T. K. Maji, G. Mostafa, T.-H. Lub and N. R. Chaudhuri *New J. Chem.*, 2003, **27**, 185-187; N. L. Rosi, M. Eddaoudi, J. Kim, M. O'Keeffe, O. M. Yaghi, *CrystEngComm*, 2002, **4**, 401-404; F. A. Cotton, C. Lin and C. A. Murillo, *J. Chem. Soc., Dalton Trans.*, 2001, 499-501; M. E. Braun, C. D. Steffek, J. Kim, P. G. Rasmussen and O. M. Yaghi, *Chem. Commun.* 2001, 2532-2533; M. O'Keeffe, M. Eddaoudi, H. Li, T. Reineke and O. M. Yaghi, *J. Solid State Chem.*, 2000, **152**, 3-20.
- 3 M. Arca, A. Cornia, F. A. Devillanova, A. C. Fabretti, F. Isaia, V. Lippolis and G. Verani, *G. Inorg. Chim. Acta* **1997**, **262**, 81-84.
 - 4 K. Biradha, M. Sarkar and L. Rajput, *Chem. Commun.*, **2006**, 4169-4179.
 - 5 M. C. Aragoni, M. Arca, F. Demartin, F.A. Devillanova, C. Graiff, F. Isaia, V. Lippolis, A. Tiripicchio and G. Verani, *J. Chem. Soc., Dalton Trans.* 2001, 2671-2677.
 - 6 I. Haiduc, *Handbook of Chalcogen Chemistry*, F. A. Devillanova ed., Royal Society of Chemistry, 2006, 593-643.
 - 7 M. C. Aragoni, M. Arca, N.R. Champness, A.V. Chernikov, F.A. Devillanova, F. Isaia, V. Lippolis, N.S. Oxtoby, G. Verani, S.Z. Vatsadze and C. Wilson, *Eur. J. Inorg. Chem.*, 2004, **10**, 2008-2012.
 - 8 M. C. Aragoni, M. Arca, N.R. Champness, M. De Pasquale, F.A. Devillanova, F. Isaia, V. Lippolis, N.S. Oxtoby and C. Wilson, *CrystEngComm*, 2005, **7**, 363-369.
 - 9 M. Crespo Alonso, M. Arca, F. Isaia, R. Lai, V. Lippolis, S. K. Callear, M. Caricato, D. Pasini, S. J. Coles and M. C. Aragoni, *CrystEngComm*, 2014, **16**, 8582-8590.
 - 10 M. C. Aragoni, M. Arca, C. Caltagirone, C. Castellano, F. Demartin, A. Garau, F. Isaia, V. Lippolis, R. Montis and A. Pintus, *CrystEngComm*, 2012, **14**, 5809-5823.
 - 11 P. Porta, A. Sgamellotti, N. Vinciguerra, *Inorg. Chem.*, 1968, **7**, 2625-2629.
 - 12 G. M. Sheldrick, SHELX suite of programs for crystal structure solution and refinement, Univ. of Göttingen, Germany, 1997.
 - 13 G. M. Sheldrick, *Acta Cryst.* **2008**, **A64**, 112-122.
 - 14 G. M. Sheldrick, SADABS V2.10, University of Göttingen, 2003.
 - 15 Oxford Diffraction Ltd., Version 1.171.32.5 (release 08-05-2007 CrysAlis171 .NET).
 - 16 C. J. Cramer, in *Essentials of Computational Chemistry*, Chapter 8, 2nd Ed., Wiley, Chichester, England, 2004.
 - 17 Gaussian 09, Revision A.02, M. J. Frisch, G. W. Trucks, H. B. Schlegel, G. E. Scuseria, M. A. Robb, J. R. Cheeseman, G. Scalmani, V. Barone, B. Mennucci, G. A. Petersson, H. Nakatsuji, M. Caricato, X. Li, H. P. Hratchian, A. F. Izmaylov, J. Bloino, G. Zheng, J. L. Sonnenberg, M. Hada, M. Ehara, K. Toyota, R. Fukuda, J. Hasegawa, M. Ishida, T. Nakajima, Y. Honda, O. Kitao, H. Nakai, T. Vreven, J. A. Montgomery, Jr., J. E. Peralta, F. Ogliaro, M. Bearpark, J. J. Heyd, E. Brothers, K. N. Kudin, V. N. Staroverov, R. Kobayashi, J. Normand, K. Raghavachari, A. Rendell, J. C. Burant, S. S. Iyengar, J. Tomasi, M. Cossi, N. Rega, J. M. Millam, M. Klene, J. E. Knox, J. B. Cross, V. Bakken, C. Adamo, J. Jaramillo, R. Gomperts, R. E. Stratmann, O. Yazyev, A. J. Austin, R. Cammi, C. Pomelli, J. W. Ochterski, R. L. Martin, K. Morokuma, V. G. Zakrzewski, G. A. Voth, P. Salvador, J. J. Dannenberg, S. Dapprich, A. D. Daniels, Ö. Farkas, J. B. Foresman, J. V. Ortiz, J. Cioslowski, and D. J. Fox, Gaussian, Inc., Wallingford CT, 2009.
 - 18 C. Adamo and V. Barone, *J. Chem. Phys.*, 1998, **108**, 664-675.
 - 19 A. Schäfer, H. Horn and R. Ahlrichs, *J. Chem. Phys.*, 1992, **97**, 2571-2577.
 - 20 (a) G. Schaftenaar and J. H. Noordik, *J. Comput.-Aided Mol. Des.*, 2000, **14**, 123-134; (b) R. Dennington, T. Keith and J. Millan, GaussView, Ver. 5.08, Semichem Inc., Shawee Mission Ks, 2009.
 - 21 R. I. Meltzer, A. D. Lewis and J. A. King, *J. Chem. Am. Soc.*, 1955, **77**, 4062-4066.
 - 22 I. Ondrejčková, R. Uhrecký, M. Koman, Z. Faberová, D. Lacková, J. Mrozinsky, B. Kalínská and Z. Padelková, *Inorg. Chim. Acta*, 2014, **414**, 33-38.

Coordination polymers and polygons using di-pyridyl-thiadiazole spacers and substituted phosphorodithioato NiII complexes: potential and limitations for inorganic crystal engineering

M. C. Aragoni, M. Arca, S. J. Coles, M. Crespo, S. L. Coles (née Huth), R. P. Davies, M. B. Hursthouse, F. Isaia, R. Lai, V. Lippolis



Differently P-substituted phosphorodithioato NiII complexes were reacted with bis-pyridyl thiadiazole spacers L1 and L2 differing for the position of the donor atoms obtaining either polymeric or discrete supramolecular constructs.